NAMT
93-003

Numerical Solution of Diffraction Problems: A Method of Variation of Boundaries III. Doubly Periodic Gratings

Oscar P. Bruno
Georgia Institute of Technology

Fernando Reitich
Carnegie Mellon University

Research Report No. 93-NA-003

January 1993

Sponsors

U.S. Army Research Office
Research Triangle Park
NC 27709

National Science Foundation
1800 G Street, N.W.
Washington, DC 20550

Numerical solution of diffraction problems: a method of variation of boundaries III. Doubly periodic gratings

Oscar P. Bruno* Fernando Reitich†

Abstract

We present a new numerical method for the solution of the problem of diffraction of light by a doubly periodic surface. This method is based on a high order rigorous perturbative technique, whose application to singly periodic gratings was treated in the first two papers of this series. We briefly discuss the theoretical basis of our algorithm, namely, the property of analyticity of the diffracted fields with respect to variations of the interfaces. While the algebraic derivation of some basic recursive formulae is somewhat involved, it results in expressions which are easy to implement numerically.

We present a variety of numerical examples (for bi-sinusoidal gratings), in order to demonstrate the accuracy exhibited by our method as well as its limited requirements in terms of computing power. Generalization of our computer code to crossed gratings other than bi-sinusoidal is in principle immediate, but the full domain of applicability of our algorithm remains to be explored. Comparison with results presented previously for actual experimental configurations shows a substantial improvement in the resolution of our numerics over that given by other methods introduced in the past.

*School of Mathematics, Georgia Institute of Technology, Atlanta, Georgia 30332-0160
†Department of Mathematics, Carnegie Mellon University, Pittsburgh, Pennsylvania 15213-3890

1 Introduction

Diffraction gratings are optical devices which, due in part to their microscopic geometrical design, can produce useful patterns of diffraction of electromagnetic radiation, and can exhibit good properties of absorption of electromagnetic energy. Because of their theoretical interest, as well as their engineering and industrial applications, a great deal of effort has been devoted to theoretical and experimental investigation of these devices. Most such investigations (including the first two papers [5, 6] in this series) have dealt with *singly periodic gratings*, sometimes called *classical gratings*, even though the corresponding *doubly periodic* structures, or *crossed gratings*, hold much interest also [14, 24, 16, 8, 11, 15, 18]. Indeed, not only can crossed gratings be used in settings in which classical gratings are employed, but they are also natural candidates as good absorbers of solar energy or as anti-reflecting surfaces.

Diffraction gratings give rise to complicated physical phenomena, and their experimental investigation is costly. Thus, numerical methods capable of solving Maxwell's equations and producing accurate predictions of their properties play an important role. Methods that produce satisfactory results for classical gratings have been introduced in the last few decades [22], see also [6]. Numerical methods for crossed gratings, based on integral or differential formalisms, have also been given [16, 24, 8, 18, 19, 12], and, together with some experimental research [18], have helped gain some insight into their properties. It is recognized [15, p. 57], however, that improvement in the numerical modeling of crossed gratings is necessary. Indeed, the mathematical complexities introduced by the oscillatory nature of the waves and interfaces which already exist in the singly periodic case, are amplified in the case of crossed gratings in which a three-dimensional diffraction problem must be solved. These difficulties lead to long computing time and limited resolution in the computer codes produced until now.

In this paper we shall introduce a new numerical algorithm for the solution of doubly periodic diffraction problems. This algorithm is based on a rigorous high order perturbative technique which we introduced recently in the context of singly periodic problems [5, 6]. For classical gratings we have shown, through applications to sinusoidal and triangular profiles, that perturbative techniques can lead to results of considerable better quality than the integral or differential formalisms in many situations of interest in applications. The success of our algorithm in the singly periodic case motivated us to extend our methods to the case of crossed gratings. As it happens, the three dimensional version of our algorithm yields a very good performance; some examples will be given below. Since doubt had been cast [23, p. 411] on the theoretical validity of perturbation methods, such as ours, in diffraction problems, we produced [4] a detailed analysis establishing, in the singly periodic case, a rigorous justification of our numerical approach. The extension of the theory to the three dimensional problem will be briefly discussed in §3.1. It follows along the same lines of [4], though some points of difficulty do occur. The basic formulae of the algorithm are presented in §3.2 and numerical experiments follow in §4.

While our method applies to general bi-periodic surfaces, our numerical experiments will be confined, for simplicity and following [18], to surfaces which consist of the sum of two sinusoids. Generalization of our computer code to surfaces other than bi-sinusoidal is in principle immediate, but the full domain of applicability of our algorithm is yet to be explored. Comparison with previous work will show that the use of our perturbative approach can be very advantageous. For example for a bi-sinusoidal gold grating for which numerical and experimental data is presented in [18], we obtain results with almost full double precision accuracy, while results with an accuracy of eight digits are already obtained by a twenty second calculation in a desk top computer. The accuracy of the integral method has been estimated to be, in the same problem, of about two digits [8]. This is a particularly simple case, and the accuracy of our algorithm, (as that given by other methods) decreases when the height to period ratio of the grating is increased. We will demonstrate, however, that our algorithm can be applied to wide range experimental configurations with a rather limited computational effort, and that, at least in the cases considered here, it yields results of substantially better definition than other methods available at present.

2 Doubly periodic gratings

Consider a doubly periodic grating, i.e., a surface

$$z = f(x, y),$$

and regions $\Omega^+ = \{z > f(x,y)\}$ and $\Omega^- = \{z < f(x,y)\}$ which are assumed to be filled by two different materials, such as air and a metal, of respective dielectric constants ϵ^+ and ϵ^-. The permeability of both materials is assumed to equal μ_0, the permeability of vacuum. If the function f does not depend on y, then we have a singly periodic grating. In this paper, however, we consider the case in which the grating is genuinely doubly periodic, with periods d_1 and d_2 in the x and y directions, respectively.

We wish to determine the pattern of diffraction that occurs when an electromagnetic plane wave

$$\vec{E}^i = \vec{A}e^{i(\alpha x+\beta y-\gamma z-i\omega t)}$$
$$\vec{H}^i = \vec{B}e^{i(\alpha x+\beta y-\gamma z-i\omega t)}$$

illuminates the grating. Here we have

$$\vec{A}\cdot\vec{k} = 0 \text{ and } \vec{B} = \frac{1}{\omega\mu_0}\vec{k}\times\vec{A}, \tag{1}$$

where

$$\vec{k} = (\alpha, \beta, -\gamma)$$

is the wave vector.

Dropping the factor $e^{-i\omega t}$, the time harmonic Maxwell equations for the total fields read

$$\begin{aligned} \nabla\times\vec{E} = i\omega\mu_0\vec{H} \ &, \ \nabla\cdot\vec{E} = 0 \ , \\ \nabla\times\vec{H} = -i\omega\epsilon\vec{E} \ &, \ \nabla\cdot\vec{H} = 0 \ . \end{aligned} \tag{2}$$

In particular, the fields $v = \vec{E}, \vec{H}$ satisfy the Helmholtz equation

$$\Delta v + k^2 v = 0 \tag{3}$$

with $k^2 = \omega^2\epsilon\mu_0$

The total fields

$$\vec{E}^{up} = \vec{E}^i + \vec{E}^+ \quad , \quad \vec{H}^{up} = \vec{H}^i + \vec{H}^+$$
$$\vec{E}^{down} = \vec{E}^- \quad , \quad \vec{H}^{down} = \vec{H}^-$$

must satisfy these equations in the regions Ω^+ and Ω^-, and at the interface $z = f(x,y)$ they must verify the transmission conditions

$$n \times (\vec{E}^{up} - \vec{E}^{down}) = 0 \ , \ n \times (\vec{H}^{up} - \vec{H}^{down}) = 0 \text{ on } z = f(x,y). \qquad (4)$$

In case the region Ω^- is filled by a perfect conductor, there will only be reflected fields. The boundary condition in this case is

$$n \times \vec{E}^{up} = 0 \text{ on } z = f(x,y) \ .$$

To complete the prescriptions, we observe that the double-periodicity of the structure implies that the fields must be (α,β) quasi-periodic, i.e., they must verify equations of the form

$$v(x+d_1,y,z) = e^{i\alpha d_1} v(x,y,z) \text{ and } v(x,y+d_2,z) = e^{i\beta d_2} v(x,y,z),$$

and, finally, that the diffracted fields must consist of outgoing waves.

By separation of variables it is easy to show that the diffracted electric field in the regions $z > \max\{f(x,y)\}$ and $z < \min\{f(x,y)\}$ is given by the expansions

$$\vec{E}^{\pm} = \sum_{r=-\infty}^{\infty} \sum_{s=-\infty}^{\infty} \vec{B}^{\pm}_{r,s} e^{i\alpha_r x + i\beta_s y \pm i\gamma^{\pm}_{r,s} z} \qquad (5)$$

respectively. Here,

$$\alpha_r = \alpha + rK_1 \ , \ \beta_s = \beta + sK_2 \ , \ \alpha_r^2 + \beta_s^2 + (\gamma^{\pm}_{r,s})^2 = (k^{\pm})^2 \qquad (6)$$

where $\gamma^{\pm}_{r,s}$ is determined by $\mathrm{Im}(\gamma^{\pm}_{r,s}) > 0$ or $\gamma^{\pm}_{r,s} \geq 0$,

$$(k^{\pm})^2 = \omega^2 \epsilon^{\pm} \mu_0$$

and

$$K_1 = \frac{2\pi}{d_1} \ , \ K_2 = \frac{2\pi}{d_2}.$$

It is clear from (6) that only a finite number of modes propagate away from the grating, the remaining modes decaying exponentially with the distance to the surface. The quantities of interest are the *grating efficiencies*

$$e^{\pm}_{r,s} = \frac{|B^{\pm}_{r,s}|^2 \gamma^{\pm}_{r,s}}{\gamma^{+}_{0,0}} \tag{7}$$

for the finitely many propagating modes, i.e. the modes (r, s) such that $\gamma^{\pm}_{r,s}$ is real.

In this connection, the principle of conservation of energy yields a simple and valuable test of accuracy for numerical methods in diffraction problems in the absence of lossy materials: if we let $U^{\pm}$ denote the set of indices corresponding to the non-evanescent modes, then

$$\sum_{(r,s)\in U^{+}} e^{+}_{r,s} + \sum_{(r,s)\in U^{-}} e^{-}_{r,s} = 1, \tag{8}$$

provided the dielectric constants ϵ^{+} and ϵ^{-} are real.

3 Solution via variation of boundaries

In §3.1 we present a brief account of the theory upon which our numerical method is based and in §3.2 we derive the basic recursive formulae. The derivation of these formulae is rather lengthy, but it results in expressions which are easy to implement numerically.

3.1 Three-dimensional theory

In this section we shall describe the main theoretical results of analyticity of the solution $(\vec{E}(x, y, z; \delta), \vec{H}(x, y, z; \delta))$ corresponding to the grating

$$z = \delta f(x, y)$$

with respect to the height δ. Proofs will only be outlined; details will appear elsewhere. The reader can also consult our work [4] where the two-dimensional problem was studied. Even though the proof in the three-dimensional case follows the same lines, some points of difficulty do occur due to the higher dimensionality and the vector-valued character of Maxwell's equations (in contrast with the scalar Helmholtz equation of the two-dimensional case). As in [4], the basic idea is to study a *holomorphic* formulation of the problem using surface potentials. The first step consists of showing that the densities entering the potential theoretic formulation are analytic in the parameter δ as well as in the spatial variables. The analyticity of the densities allows us then to show that, for sufficiently small δ, the solutions $(\vec{E}^+(x,y,z;\delta), \vec{H}^+(x,y,z;\delta))$ and $(\vec{E}^-(x,y,z;\delta), \vec{H}^-(x,y,z;\delta))$ extend analytically (in (x,y,z,δ)) to $\{\, z > z_0 \,\}$ and $\{\, z < -z_0 \,\}$ respectively, where $z_0 < 0$ is sufficiently small. This, in turn gives the theoretical justification for the recursive formulae in §3.2: the partial derivatives of $(\vec{E}^\pm(x,y,z;\delta), \vec{H}^\pm(x,y,z;\delta))$ with respect to δ at $\delta = 0$ ("flat interface") satisfy certain boundary value problems for Maxwell's equations, in regions with plane boundaries which can be solved in closed form. Moreover, as a byproduct of the proof of analytic continuation of the fields we establish their analyticity *away* from the interface *without a restriction on the size of* δ. In particular, this implies that the Rayleigh coefficients $\vec{B}^\pm_{r,s} = \vec{B}^\pm_{r,s}(\delta)$ are analytic functions of δ *for* δ *in a complex neighborhood of the real line*. Thus, one can use *Padé approximants* to extract the values of the Rayleigh coefficients from their Taylor expansions, even beyond their radii of convergence; see §4.

As we said above, the starting point for the proofs is a potential theoretic formulation, see also [9, 10]. Motivated by the representation formula ([20, p. 160])

$$
\begin{aligned}
\vec{E}(x,y,z) &= \int_F \left[i\omega\mu j\Phi - j' \times \nabla\Phi + \frac{1}{i\omega\epsilon}\mathrm{Div}(j)\nabla\Phi \right] d\sigma(x',y',z'), \\
\vec{H}(x,y,z) &= \int_F \left[i\omega\epsilon j'\Phi + j \times \nabla\Phi + \frac{1}{i\omega\mu}\mathrm{Div}(j')\nabla\Phi \right] d\sigma(x',y',z')
\end{aligned}
$$

we seek a solution $(E^\pm, H^\pm)$ in the form

$$
\begin{aligned}
\vec{E}^\pm(x,y,z;\delta) &= -\mu_0\mathcal{D}^\pm_\delta(j') + \epsilon^\pm i\omega\mu_0\mathcal{S}^\pm_\delta(j) - \frac{1}{i\omega}\mathcal{T}^\pm_\delta(j) \qquad (9) \\
\vec{H}^\pm(x,y,z;\delta) &= \epsilon^\pm\mathcal{D}^\pm_\delta(j) + \epsilon^\pm i\omega\mu_0\mathcal{S}^\pm_\delta(j') - \frac{1}{i\omega}\mathcal{T}^\pm_\delta(j')
\end{aligned}
$$

where the operators $\mathcal{D}_\delta^\pm$, $\mathcal{S}_\delta^\pm$, $\mathcal{T}_\delta^\pm$ are defined by

$$\begin{aligned}
\mathcal{D}_\delta^\pm(j')(x,y,z) &= \nabla\times\int_0^{d_1}\int_0^{d_2}\Phi^\pm(x-x',y-y',z-\delta f(x',y'))j'(x',y') \\
&\qquad (1+(\delta f_x(x',y'))^2+(\delta f_y(x',y'))^2)^{1/2}\,dx'\,dy' \\
\mathcal{S}_\delta^\pm(j)(x,y,z) &= \int_0^{d_1}\int_0^{d_2}\Phi^\pm(x-x',y-y',z-\delta f(x',y'))j(x',y') \\
&\qquad (1+(\delta f_x(x',y'))^2+(\delta f_y(x',y'))^2)^{1/2}\,dx'\,dy' \\
\mathcal{T}_\delta^\pm(j)(x,y,z) &= \nabla\int_0^{d_1}\int_0^{d_2}\Phi^\pm(x-x',y-y',z-\delta f(x',y'))\mathrm{Div}(j)(x',y') \\
&\qquad (1+(\delta f_x(x',y'))^2+(\delta f_y(x',y'))^2)^{1/2}\,dx'\,dy'\,.
\end{aligned}$$

Here j and j' are quasi-periodic surface currents, i.e. if $n_\delta = n_\delta(x,y)$ is the unit normal vector to $\{\,z=\delta f(x,y)\,\}$ at $(x,y,\delta f(x,y))$ (directed towards $\{\,z<\delta f(x,y)\,\}$)

$$j\cdot n_\delta = j'\cdot n_\delta = 0;$$

$\mathrm{Div}(j)$ denotes the surface divergence (see [20, pp. 154, 157]) of the function j, and the functions $\Phi^\pm$ denote the quasi-periodic fundamental solutions of Helmholtz' equation (3). We have chosen the constants that multiply the operators in (9) in such a way that the highest order singularity in the resulting integral equations (equations (11) below) cancels out. As for the quasi-periodic fundamental solution, we have, formally,

$$\Phi^\pm(x,y,z) = \frac{i}{2d_1d_2}\sum_{r=-\infty}^{\infty}\sum_{s=-\infty}^{\infty}\frac{1}{\gamma_{r,s}^\pm}e^{i\alpha_r x+i\beta_s y+i\gamma_{r,s}^\pm|z|}\,. \tag{10}$$

Using the expansion (10) and the fact (see [4]) that

$$\frac{i}{2d_2}\sum_{s=-\infty}^{\infty}\frac{1}{\gamma_{r,s}^\pm}e^{i\beta_s y+i\gamma_{r,s}^\pm|z|} = \frac{i}{4}\sum_{s=-\infty}^{\infty}e^{-is\beta d_2}H_0^{(1)}[(\sqrt{(k^\pm)^2-\alpha_r^2})|(y+sd_2,z)|]$$

(where $H_0^{(1)}$ denotes a Hankel function) together with certain symmetry related relations, the existence of an (α, β) quasi-periodic fundamental solution can rigorously be established.

Now, using the *jump relations* for the operators $\mathcal{D}_\delta^\pm$, $\mathcal{S}_\delta^\pm$ and $\mathcal{T}_\delta^\pm$ (see [20, p. 205]), the transmission conditions (4) imply

$$\begin{aligned} -\mu_0 j' &- \mu_0 n_\delta \times \left[\mathcal{D}_\delta^+(j') - \mathcal{D}_\delta^-(j')\right] + i\omega\mu_0 n_\delta \times \left[\epsilon^+ \mathcal{S}_\delta^+(j) - \epsilon^- \mathcal{S}_\delta^-(j)\right] \\ &- \frac{1}{i\omega} n_\delta \times \mathcal{R}_\delta(j) = -n_\delta \times \vec{E}^i \quad \text{on } [0, d_1] \times [0, d_2] \end{aligned} \tag{11}$$

$$\begin{aligned} \frac{(\epsilon^+ + \epsilon^-)}{2} j &+ n_\delta \times \left[\epsilon^+ \mathcal{D}_\delta^+(j) - \epsilon^- \mathcal{D}_\delta^-(j)\right] + i\omega\mu_0 n_\delta \times \left[\epsilon^+ \mathcal{S}_\delta^+(j') - \epsilon^- \mathcal{S}_\delta^-(j')\right] \\ &- \frac{1}{i\omega} n_\delta \times \mathcal{R}_\delta(j') = -n_\delta \times \vec{H}^i \quad \text{on } [0, d_1] \times [0, d_2] \end{aligned}$$

where

$$\begin{aligned} \mathcal{D}_\delta^\pm(j')(x,y) &= \mathcal{D}_\delta^\pm(j')(x, y, \delta f(x,y)) \\ \mathcal{S}_\delta^\pm(j)(x,y) &= \mathcal{S}_\delta^\pm(j)(x, y, \delta f(x,y)) \end{aligned}$$

$$\begin{aligned} \mathcal{R}_\delta(j)(x,y) &= \int_0^{d_1}\int_0^{d_2} (j(x',y') \cdot \nabla_{x',y'}) \nabla_{x',y'} (\Phi^+(x-x', y-y', \delta f(x,y) - \delta f(x',y')) \\ &- \Phi^-(x-x', y-y', \delta f(x,y) - \delta f(x',y')) \\ &\quad (1 + (\delta f_x(x',y'))^2 + (\delta f_y(x',y'))^2)^{1/2}\, dx'\, dy' \end{aligned}$$

(In deriving the above equations we used the formula of integration by parts

$$\int_F U \mathrm{Div}(V) + \int_F V \cdot \mathrm{Grad}(U) = 0$$

where $\mathrm{Grad}(U)$ denotes the surface gradient of the function U, i.e.

$$\nabla U = \mathrm{Grad}(U) + n_\delta \frac{\partial U}{\partial n_\delta};$$

see [20, p. 163]).

Defining

$$\mathcal{A}_\delta = \begin{bmatrix} n_\delta \times \left(\mathcal{D}_\delta^+ - \mathcal{D}_\delta^-\right) & -i\omega n_\delta \times \left(\epsilon^+ \mathcal{S}_\delta^+ - \epsilon^- \mathcal{S}_\delta^-\right) + \frac{1}{i\omega\mu_0} n_\delta \times \mathcal{R}_\delta \\ \frac{2}{\epsilon^+ + \epsilon^-}\left[i\omega\mu_0 n_\delta \times \left(\epsilon^+ \mathcal{S}_\delta^+ - \epsilon^- \mathcal{S}_\delta^-\right) - \frac{1}{i\omega\mu_0} n_\delta \times \mathcal{R}_\delta\right] & \frac{2}{\epsilon^+ + \epsilon^-} n_\delta \times \left(\epsilon^+ \mathcal{D}_\delta^+ - \epsilon^- \mathcal{D}_\delta^-\right) \end{bmatrix}$$

the integral equations (11) can be written as

$$(I + \mathcal{A}_\delta)(J)(x,y) = F_\delta(x,y)$$

where

$$J(x,y) = \begin{bmatrix} j'(x,y) \\ j(x,y) \end{bmatrix} \quad \text{and}$$

$$F_\delta(x,y) = \begin{bmatrix} \frac{1}{\mu_0} n_\delta \times \vec{E}^i(x,y,\delta f(x,y)) \\ -\frac{2}{\epsilon^+ + \epsilon^-} n_\delta \times \vec{H}^i(x,y,\delta f(x,y)) \end{bmatrix}.$$

A close look at the operator $\mathcal{A}_\delta$ reveals that the kernels are only weakly singular. Indeed, the kernel in $\mathcal{R}_\delta$ has a singularity of the order $|(x-x', y-y')|^{-1}$, due to a cancellation mentioned above, while the same is true for $n_\delta \times \mathcal{D}_\delta^\pm$ as can be seen from the equality

$$\begin{gathered} n_\delta \times (\nabla\Phi^\pm \times j')(x-x', y-y', \delta f(x,y) - \delta f(x',y')) = \\ [(n_\delta(x,y) - n_\delta(x',y')) \cdot j']\, \nabla\Phi^\pm - \frac{\partial\Phi^\pm}{\partial n_\delta(x,y)} j'. \end{gathered}$$

Moreover, it can shown that for each fixed $\delta_0 \in \mathbb{R}$ there exist positive numbers ϵ and ν such that the operator $\mathcal{A}_\delta$ maps the (Banach) space

$$\begin{aligned} \mathcal{J}_{\epsilon,\nu}(\delta_0) = \Big\{ J(x,y;\delta) = \begin{bmatrix} j'(x,y;\delta) \\ j(x,y;\delta) \end{bmatrix} &: J(\cdot;\delta) \text{ is } (\alpha,\beta)-\text{quasi-periodic}, \\ &\text{analytic for } |\mathrm{Im}(x)| < \nu,\ |\mathrm{Im}(y)| < \nu,\ |\delta - \delta_0| < \epsilon \text{ and} \\ &\text{continuous for } |\mathrm{Im}(x)| \le \nu,\ |\mathrm{Im}(y)| \le \nu,\ |\delta - \delta_0| \le \epsilon \Big\} \end{aligned}$$

into itself, continuously in the norm

$$\|J\|_{\mathcal{J}} = \sup\{\,|J(x,y;\delta)| \,:\, |\mathrm{Im}(x)| \le \nu\,,\, |\mathrm{Im}(y)| \le \nu\,,\, |\delta-\delta_0| \le \epsilon\}\,.$$

(Note that this says that, provided the currents are analytic, the integrals in (11) define analytic functions of $(x, y; \delta)$, *even though the kernels are not themselves analytic*). Finally, for each fixed $\delta_0 \in \mathbf{R}$, the operator $\mathcal{A}_{\delta_0}$ can be shown to be *compact*. Thus, the operator $I + \mathcal{A}_{\delta_0}$ is invertible, *provided the solution to the problem when $\delta = \delta_0$ is unique*. If this is the case, then a simple perturbation argument shows that the operator $I + \mathcal{A}_\delta$ is invertible in $\mathcal{J}_{\epsilon,\nu}(\delta_0)$ for δ close to δ_0.

The invertibility of $I + \mathcal{A}_\delta$ implies that the surface currents j and j' defined by (11) are analytic functions of $(x, y; \delta)$. This, in turn, allows us to prove the following Theorem.

Theorem 1 *Fix $\delta_0 \in \mathbf{R}$ and let $(\vec{E}^\pm(x,y,z;\delta_0), \vec{H}^\pm(x,y,z;\delta_0))$ denote a solution to (2) that consists of outgoing waves and satisfies (4) on $z = \delta_0 f(x,y)$. Assume that this solution is unique (which implies that the solution $(\vec{E}^\pm(x,y,z;\delta), \vec{H}^\pm(x,y,z;\delta))$ corresponding to the grating $z = \delta_0 f(x,y)$ is also unique for δ near δ_0). Then*

(i) *If $z_0 > \delta_0 \max|f|$ ($z_0 < \delta_0 \min|f|$), there exists $\epsilon_0 = \epsilon_0(\delta_0, z_0)$ such that $(\vec{E}^+(x,y,z;\delta), \vec{H}^+(x,y,z;\delta))$ $((\vec{E}^-(x,y,z;\delta), \vec{H}^-(x,y,z;\delta)))$ is analytic in $(x,y,z;\delta)$ for $|\delta-\delta_0| < \epsilon_0$ and $|z - z_0| < \epsilon_0$.*

(ii) *The functions $n_\delta(x,y) \times \vec{E}^\pm(x,y,\delta f(x,y);\delta)$ and $n_\delta(x,y) \times \vec{H}^\pm(x,y,\delta f(x,y);\delta)$ are analytic in (x,y,δ) for δ near δ_0.*

(iii) *Given $\delta_0 \in \mathbf{R}$ there exists $\epsilon_1 > 0$ such that $(\vec{E}^\pm(x,y,z;\delta), \vec{H}^\pm(x,y,z;\delta))$ are analytic for $|\delta - \delta_0| < \epsilon_1$ and $|z - \delta_0 f(x,y)| < \epsilon_1$.*

Note that the last statement implies that the fields can be extended as analytic functions of $(x,y,z;\delta)$ even as the surface $z = \delta f(x,y)$ passes over the point (x,y,z) due to variations in δ. It is also to be noted that the assumed uniqueness holds trivially for $\delta_0 = 0$.

3.2 Recursive Formulae

Besides its independent theoretical interest, the result quoted above has proved significant in practice as we have found that the the analyticity properties of the fields can be exploited in their numerical evaluation. In what follows we shall derive recursive formulae for the Taylor coefficients

$$\vec{d}^{\pm}_{k,(r,s)} = \begin{bmatrix} d^{1,\pm}_{k,(r,s)} \\ d^{2,\pm}_{k,(r,s)} \\ d^{3,\pm}_{k,(r,s)} \end{bmatrix}$$

of the Rayleigh amplitudes $\vec{B}^{\pm}_{r,s}$ of $\vec{E}$ (cf. (5)):

$$\vec{B}^{\pm}_{r,s}(\delta) = \sum_{k=0}^{\infty} \vec{d}^{\pm}_{k,(r,s)} \delta^k . \tag{12}$$

Once $\vec{E}$ has been obtained, the magnetic field is given by

$$\vec{H} = \frac{1}{i\omega\mu_0}(\nabla \times \vec{E}) .$$

The recursive formulae will be derived by differentiation of the transmission conditions

$$\begin{aligned} n_\delta \times (\vec{E}^+ - \vec{E}^-) &= -(n_\delta \times \vec{A}) e^{i(\alpha x + \beta y - \gamma\delta f(x,y))} \\ n_\delta \times (\vec{H}^+ - \vec{H}^-) &= -(n_\delta \times \vec{B}) e^{i(\alpha x + \beta y - \gamma\delta f(x,y))} \text{ on } z = \delta f(x,y) \end{aligned} \tag{13}$$

with respect to δ. Such differentiations are justified by Theorem 1. The algebra required by this derivation is quite involved, and we have chosen to present it in detail. This complication can only be considered as a minor drawback, however, as the resulting formulae are rather simple, and can easily be implemented numerically.

To obtain these formulae, first notice that, due to (2), we have that

$$\nabla \cdot \vec{E}^{\pm} = 0 \quad \text{in } \pm z > \pm\delta f(x,y) \tag{14}$$

and that equations (13) are equivalent to

$$\begin{aligned} n_\delta \times (\vec{E}^+ - \vec{E}^-) &= -(n_\delta \times \vec{A}) e^{i(\alpha x + \beta y - \gamma\delta f(x,y))} \\ n_\delta \times (\nabla \times \vec{E}^+ - \nabla \times \vec{E}^-) &= -i\omega\mu_0 (n_\delta \times \vec{B}) e^{i(\alpha x + \beta y - \gamma\delta f(x,y))} \text{ on } z = \delta f(x,y). \end{aligned} \tag{15}$$

Now, using

$$n_\delta = n_\delta(x,y) = \frac{1}{\sqrt{1+\delta^2 f_x(x,y)^2+\delta^2 f_y(x,y)^2}}(-\delta f_x(x,y), -\delta f_y(x,y), 1)$$

together with equation (1), we can rewrite (15) in the form

$$\begin{aligned}
&(-\delta f_x(x,y), -\delta f_y(x,y), 1) \times \left(\vec{E}^+(x,y,\delta f(x,y);\delta) - \vec{E}^-(x,y,\delta f(x,y);\delta)\right) \\
&\qquad = -\left((-\delta f_x(x,y), -\delta f_y(x,y), 1) \times \vec{A}\right) e^{i(\alpha x+\beta y-\gamma\delta f(x,y))} \qquad (16) \\
&(-\delta f_x(x,y), -\delta f_y(x,y), 1) \times \left(\nabla\times\vec{E}^+(x,y,\delta f(x,y);\delta) - \nabla\times\vec{E}^-(x,y,\delta f(x,y);\delta)\right) \\
&\qquad = -i\left((-\delta f_x(x,y), -\delta f_y(x,y), 1) \times (\vec{k}\times\vec{A})\right) e^{i(\alpha x+\beta y-\gamma\delta f(x,y))}\,.
\end{aligned}$$

Only four of the six relations (16) are independent; a set of four *independent* equations is

$$\begin{aligned}
E^{2,+} - E^{2,-} + \delta f_y(E^{3,+} - E^{3,-}) &= -(A^2+\delta f_y A^3) e^{i(\alpha x+\beta y-\gamma\delta f(x,y))} \\
E^{1,+} - E^{1,-} + \delta f_x(E^{3,+} - E^{3,-}) &= -(A^1+\delta f_x A^3) e^{i(\alpha x+\beta y-\gamma\delta f(x,y))} \\
(E_z^{1,+} - E_z^{1,-}) - (E_x^{3,+} - E_x^{3,-}) &+ \delta f_y\left[(E_x^{2,+} - E_x^{2,-}) - (E_y^{1,+} - E_y^{1,-})\right] \\
&= -i\left[-\gamma A^1 - \alpha A^3 + \delta f_y(\alpha A^2 - \beta A^1)\right] e^{i(\alpha x+\beta y-\gamma\delta f(x,y))} \\
(E_y^{3,+} - E_y^{3,-}) - (E_z^{2,+} - E_z^{2,-}) &+ \delta f_x\left[(E_x^{2,+} - E_x^{2,-}) - (E_y^{1,+} - E_y^{1,-})\right] \\
&= -i\left[\beta A^3 + \gamma A^2 + \delta f_x(\alpha A^2 - \beta A^1)\right] e^{i(\alpha x+\beta y-\gamma\delta f(x,y))}\,.
\end{aligned}$$

Together with the conditions

$$\begin{aligned}
E_x^{1,+} + E_y^{2,+} + E_z^{3,+} &= 0 \\
E_x^{1,-} + E_y^{2,-} + E_z^{3,-} &= 0 \quad \text{(cf. (14))}
\end{aligned}$$

these relations provide us with six equations for the six unknowns

$$\vec{E}^+ = \begin{bmatrix} E^{1,+} \\ E^{2,+} \\ E^{3,+} \end{bmatrix} \quad \text{and} \quad \vec{E}^- = \begin{bmatrix} E^{1,-} \\ E^{2,-} \\ E^{3,-} \end{bmatrix}$$

at the boundary. Differentiating these relations n times with respect to δ at $\delta = 0$, we get, at $\delta = 0$, $z = 0$

$$\frac{1}{n!}\frac{\partial^n(E^{2,+}-E^{2,-})}{\partial\delta^n} = -\sum_{k=0}^{n-1}\frac{f^{n-k}}{(n-k)!}\frac{\partial^{n-k}}{\partial z^{n-k}}\left(\frac{1}{k!}\frac{\partial^k(E^{2,+}-E^{2,-})}{\partial\delta^k}\right)$$

$$-f_y\sum_{k=0}^{n-1}\frac{f^{n-1-k}}{(n-1-k)!}\frac{\partial^{n-1-k}}{\partial z^{n-1-k}}\left(\frac{1}{k!}\frac{\partial^k(E^{3,+}-E^{3,-})}{\partial\delta^k}\right) - \left(A^2(-i\gamma)^n\frac{f^n}{n!} + A^3(-i\gamma)^{n-1}f_y\frac{f^{n-1}}{(n-1)!}\right)e^{i(\alpha x+\beta y)};$$

$$\frac{1}{n!}\frac{\partial^n(E^{1,+}-E^{1,-})}{\partial\delta^n} = -\sum_{k=0}^{n-1}\frac{f^{n-k}}{(n-k)!}\frac{\partial^{n-k}}{\partial z^{n-k}}\left(\frac{1}{k!}\frac{\partial^k(E^{1,+}-E^{1,-})}{\partial\delta^k}\right)$$

$$-f_x\sum_{k=0}^{n-1}\frac{f^{n-1-k}}{(n-1-k)!}\frac{\partial^{n-1-k}}{\partial z^{n-1-k}}\left(\frac{1}{k!}\frac{\partial^k(E^{3,+}-E^{3,-})}{\partial\delta^k}\right) - \left(A^1(-i\gamma)^n\frac{f^n}{n!} + A^3(-i\gamma)^{n-1}f_x\frac{f^{n-1}}{(n-1)!}\right)e^{i(\alpha x+\beta y)};$$

$$\frac{1}{n!}\frac{\partial^n}{\partial\delta^n}\left[(E_z^{1,+}-E_z^{1,-})-(E_x^{3,+}-E_x^{3,-})\right] = -\sum_{k=0}^{n-1}\frac{f^{n-k}}{(n-k)!}\frac{\partial^{n-k}}{\partial z^{n-k}}\left(\frac{1}{k!}\frac{\partial^k}{\partial\delta^k}\left[(E_z^{1,+}-E_z^{1,-})\right.\right.$$

$$\left.\left.-(E_x^{3,+}-E_x^{3,-})\right]\right) - f_y\sum_{k=0}^{n-1}\frac{f^{n-1-k}}{(n-1-k)!}\frac{\partial^{n-1-k}}{\partial z^{n-1-k}}\left(\frac{1}{k!}\frac{\partial^k}{\partial\delta^k}\left[(E_x^{2,+}-E_x^{2,-})-(E_y^{1,+}-E_y^{1,-})\right]\right)$$

$$-i\left[-(\gamma A^1+\alpha A^3)(-i\gamma)^n\frac{f^n}{n!} + (\alpha A^2-\beta A^1)(-i\gamma)^{n-1}f_y\frac{f^{n-1}}{(n-1)!}\right]e^{i(\alpha x+\beta y)}; \tag{17}$$

$$\frac{1}{n!}\frac{\partial^n}{\partial\delta^n}\left[(E_y^{3,+}-E_y^{3,-})-(E_z^{2,+}-E_z^{2,-})\right] = -\sum_{k=0}^{n-1}\frac{f^{n-k}}{(n-k)!}\frac{\partial^{n-k}}{\partial z^{n-k}}\left(\frac{1}{k!}\frac{\partial^k}{\partial\delta^k}\left[(E_y^{3,+}-E_y^{3,-})\right.\right.$$

$$\left.\left.-(E_z^{2,+}-E_z^{2,-})\right]\right) - f_x\sum_{k=0}^{n-1}\frac{f^{n-1-k}}{(n-1-k)!}\frac{\partial^{n-1-k}}{\partial z^{n-1-k}}\left(\frac{1}{k!}\frac{\partial^k}{\partial\delta^k}\left[(E_x^{2,+}-E_x^{2,-})-(E_y^{1,+}-E_y^{1,-})\right]\right)$$

$$-i\left[(\beta A^3+\gamma A^2)(-i\gamma)^n\frac{f^n}{n!} + (\alpha A^2-\beta A^1)(-i\gamma)^{n-1}f_x\frac{f^{n-1}}{(n-1)!}\right]e^{i(\alpha x+\beta y)}$$

and

$$\begin{aligned}\frac{\partial^n E_x^{1,+}}{\partial\delta^n}+\frac{\partial^n E_y^{2,+}}{\partial\delta^n}+\frac{\partial^n E_z^{3,+}}{\partial\delta^n} &= 0\\ \frac{\partial^n E_x^{1,-}}{\partial\delta^n}+\frac{\partial^n E_y^{2,-}}{\partial\delta^n}+\frac{\partial^n E_z^{3,-}}{\partial\delta^n} &= 0.\end{aligned} \tag{18}$$

It follows from (5) and (12) that

$$\frac{1}{k!}\frac{\partial^k\vec{E}^{\pm}}{\partial\delta^k}(x,y,z;0) = \sum_{r,s}\frac{1}{k!}\frac{d^k\vec{B}_{r,s}^{\pm}}{d\delta^k}(0)e^{i\alpha_r x+i\beta_s y\pm i\gamma_{r,s}^{\pm}z}$$

$$= \sum_{r,s} \vec{d}^{\pm}_{k,(r,s)} e^{i\alpha_r x + i\beta_s y \pm i\gamma^{\pm}_{r,s} z} . \tag{19}$$

Thus, substitution in (17) and (18) of the quantities $\frac{1}{k!}\frac{\partial^k \vec{E}^{\pm}}{\partial \delta^k}$ and their spatial derivatives as calculated from (19) yields the coefficients $\vec{d}^{\pm}_{n,(r,s)}$ in terms of the coefficients $\vec{d}^{\pm}_{k,(r,s)}$ with $k < n$ and the Fourier coefficients $C_{l,(p,q)}$ of $f^l/l!$

$$\frac{f(x,y)^l}{l!} = \sum_{p=-lF}^{lF} \sum_{q=-lF}^{lF} C_{l,(p,q)} e^{i(K_1 p x + K_2 q y)}. \tag{20}$$

Indeed, since

$$f_x \frac{f^{l-1}}{(l-1)!} = \sum_{-lF \le p,q \le lF} C_{l,(p,q)} (iK_1 p) e^{i(K_1 p x + K_2 q y)}$$

and

$$f_y \frac{f^{l-1}}{(l-1)!} = \sum_{-lF \le p,q \le lF} C_{l,(p,q)} (iK_2 q) e^{i(K_1 p x + K_2 q y)} ,$$

substitution in the first and third equations in (17) gives

$$\begin{aligned}
\textstyle\sum_{r,s} \left(d^{2,+}_{n,(r,s)} - d^{2,-}_{n,(r,s)}\right) e^{i(\alpha_r x + \beta_s y)} &= - \textstyle\sum_{k=0}^{n-1} \left(\sum_{-(n-k)F \le p,q \le (n-k)F} C_{n-k,(p,q)} e^{i(K_1 p x + K_2 q y)}\right) \\
&\cdot \left(\textstyle\sum_{l,m} \left((i\gamma^{+}_{l,m})^{n-k} d^{2,+}_{k,(l,m)} - (-i\gamma^{-}_{l,m})^{n-k} d^{2,-}_{k,(l,m)}\right) e^{i(\alpha_l x + \beta_m y)}\right) \\
&- \textstyle\sum_{k=0}^{n-1} \left(\sum_{-(n-k)F \le p,q \le (n-k)F} C_{n-k,(p,q)} (iK_2 q) e^{i(K_1 p x + K_2 q y)}\right) \qquad (21) \\
&\left(\textstyle\sum_{l,m} \left((i\gamma^{+}_{l,m})^{n-1-k} d^{3,+}_{k,(l,m)} - (-i\gamma^{-}_{l,m})^{n-1-k} d^{3,-}_{k,(l,m)}\right) e^{i(\alpha_l x + \beta_m y)}\right) \\
&- \left(A^2 (-i\gamma)^n \left(\textstyle\sum_{-nF \le p,q \le nF} C_{n,(p,q)} e^{i(K_1 p x + K_2 q y)}\right)\right. \\
&\left.+ A^3 (-i\gamma)^{n-1} \left(\textstyle\sum_{-nF \le p,q \le nF} C_{n,(p,q)} (iK_2 q) e^{i(K_1 p x + K_2 q y)}\right)\right) e^{i(\alpha x + \beta y)}
\end{aligned}$$

and

$$\sum_{r,s}\left[(i\gamma^+_{r,s}d^{1,+}_{n,(r,s)}+i\gamma^-_{r,s}d^{1,-}_{n,(r,s)})-(i\alpha_r d^{3,+}_{n,(r,s)}-i\alpha_r d^{3,-}_{n,(r,s)})\right]e^{i(\alpha_r x+\beta_s y)}$$

$$=-\sum_{k=0}^{n-1}\left(\sum_{-(n-k)F\le p,q\le(n-k)F}C_{n-k,(p,q)}e^{i(K_1px+K_2qy)}\right)\left(\sum_{l,m}\left((i\gamma^+_{l,m})^{n-k+1}d^{1,+}_{k,(l,m)}\right.\right.$$

$$\left.\left.-(-i\gamma^-_{l,m})^{n-k+1}d^{1,-}_{k,(l,m)}-(i\gamma^+_{l,m})^{n-k}(i\alpha_r)d^{3,+}_{k,(l,m)}+(-i\gamma^-_{l,m})^{n-k}(i\alpha_r)d^{3,-}_{k,(l,m)}\right)e^{i(\alpha_l x+\beta_m y)}\right)$$

$$-\sum_{k=0}^{n-1}\left(\sum_{-(n-k)F\le p,q\le(n-k)F}C_{n-k,(p,q)}(iK_2q)e^{i(K_1px+K_2qy)}\right)$$

$$\cdot\left(\sum_{l,m}\left((i\gamma^+_{l,m})^{n-k-1}(i\alpha_r)d^{2,+}_{k,(l,m)}-(-i\gamma^-_{l,m})^{n-k-1}(i\alpha_r)d^{2,-}_{k,(l,m)}\right.\right. \tag{22}$$

$$\left.\left.-(i\gamma^+_{l,m})^{n-k-1}(i\beta_s)d^{1,+}_{k,(l,m)}+(-i\gamma^-_{l,m})^{n-k-1}(i\beta_s)d^{1,-}_{k,(l,m)}\right)e^{i(\alpha_l x+\beta_m y)}\right)$$

$$-i\left[-(\gamma A^1+\alpha A^3)(-i\gamma)^n\left(\sum_{-nF\le p,q\le nF}C_{n,(p,q)}e^{i(K_1px+K_2qy)}\right)\right.$$

$$\left.+(\alpha A^2-\beta A^1)(-i\gamma)^{n-1}\left(\sum_{-nF\le p,q\le nF}C_{n,(p,q)}(iK_2q)e^{i(K_1px+K_2qy)}\right)\right]e^{i(\alpha x+\beta y)}.$$

Next, we write the Fourier series expansions for the right hand sides of (21) and (22). The right hand side of (21) is

$$-\sum_{-nF\le r,s\le nF}(A^2(-i\gamma)^n+A^3(-i\gamma)^{n-1}(iK_2s))\,C_{n,(r,s)}e^{i(\alpha_r x+\beta_s y)}$$
$$-\sum_{k=0}^{n-1}\sum_{l,m}\sum_{-(n-k)F\le p,q\le(n-k)F}\left((i\gamma^+_{l,m})^{n-k}d^{2,+}_{k,(l,m)}\right.$$

$$\left.-(-i\gamma^-_{l,m})^{n-k}d^{2,-}_{k,(l,m)}\right)C_{n-k,(p,q)}e^{i(K_1px+K_2qy)}e^{i(\alpha_l x+\beta_m y)} \tag{23}$$

$$-\sum_{k=0}^{n-1}\sum_{l,m}\sum_{-(n-k)F\le p,q\le(n-k)F}\left((i\gamma^+_{l,m}))^{n-1-k}d^{3,+}_{k,(l,m)}\right.$$

$$\left.-(-i\gamma^-_{l,m})^{n-1-k}d^{3,-}_{k,(l,m)}\right)(iK_2q)C_{n-k,(p,q)}e^{i(K_1px+K_2qy)}e^{i(\alpha_l x+\beta_m y)}$$

while the right hand side of (22) has the form

$$-i\sum_{-nF\le r,s\le nF}\left[-(\gamma A^1+\alpha A^3)(-i\gamma)^n+(\alpha A^2-\beta A^1)(-i\gamma)^{n-1}(iK_2s)\right]$$
$$\cdot C_{n,(r,s)}e^{i(\alpha_r x+\beta_s y)}-\sum_{k=0}^{n-1}\sum_{l,m}\sum_{-(n-k)F\le p,q\le(n-k)F}\left((i\gamma^+_{l,m})^{n-k+1}d^{1,+}_{k,(l,m)}\right.$$

$$-(-i\gamma^-_{l,m})^{n-k+1}d^{1,-}_{k,(l,m)} - (i\gamma^+_{l,m})^{n-k}(i\alpha_r)d^{3,+}_{k,(l,m)} + (-i\gamma^-_{l,m})^{n-k}(i\alpha_r)d^{3,-}_{k,(l,m)}\Big)$$
$$\cdot C_{n-k,(p,q)}e^{i(K_1px+K_2qy)}e^{i(\alpha_l x+\beta_m y)} - \textstyle\sum_{k=0}^{n-1}\sum_{l,m}\sum_{-(n-k)F\leq p,q\leq(n-k)F} \qquad (24)$$
$$\Big((i\gamma^+_{l,m})^{n-k-1}(i\alpha_r)d^{2,+}_{k,(l,m)} - (-i\gamma^-_{l,m})^{n-k-1}(i\alpha_r)d^{2,-}_{k,(l,m)} - (i\gamma^+_{l,m})^{n-k-1}(i\beta_s)d^{1,+}_{k,(l,m)}$$
$$+(-i\gamma^-_{l,m})^{n-k-1}(i\beta_s)d^{1,-}_{k,(l,m)}\Big)\,(iK_2q)C_{n-k,(p,q)}e^{i(K_1px+K_2qy)}e^{i(\alpha_l x+\beta_m y)}\,.$$

Now, since

$$e^{i(K_1px+K_2qy)}e^{i(\alpha_l x+\beta_m y)} = e^{i(\alpha_{p+l}x+\beta_{q+m}y)}\,,$$

changing p by $r-l$ and q by $s-m$ in the inner sums in (23) and (24) gives

$$-\textstyle\sum_{-nF\leq r,s\leq nF}\left(A^2(-i\gamma)^n + A^3(-i\gamma)^{n-1}(iK_2s)\right)C_{n,(r,s)}e^{i(\alpha_r x+\beta_s y)}$$
$$-\textstyle\sum_{k=0}^{n-1}\sum_{l,m}\sum_{l-(n-k)F\leq r\leq l+(n-k)F}\sum_{m-(n-k)F\leq s\leq m+(n-k)F}\Big[\Big((i\gamma^+_{l,m})^{n-k}d^{2,+}_{k,(l,m)}$$
$$-(-i\gamma^-_{l,m})^{n-k}d^{2,-}_{k,(l,m)}\Big) + \Big((i\gamma^+_{l,m})^{n-1-k}d^{3,+}_{k,(l,m)} - (-i\gamma^-_{l,m})^{n-1-k}d^{3,-}_{k,(l,m)}\Big)\,(iK_2(s-m))\Big]$$
$$\cdot C_{n-k,(r-l,s-m)}e^{i(\alpha_r x+\beta_s y)}$$

and

$$-i\textstyle\sum_{-nF\leq r,s\leq nF}\left[-(\gamma A^1+\alpha A^3)(-i\gamma)^n + (\alpha A^2-\beta A^1)(-i\gamma)^{n-1}(iK_2s)\right]C_{n,(r,s)}e^{i(\alpha_r x+\beta_s y)}$$
$$-\textstyle\sum_{k=0}^{n-1}\sum_{l,m}\sum_{l-(n-k)F\leq r\leq l+(n-k)F}\sum_{m-(n-k)F\leq s\leq m+(n-k)F}\Big[\Big((i\gamma^+_{l,m})^{n-k+1}d^{1,+}_{k,(l,m)}$$
$$-(-i\gamma^-_{l,m})^{n-k+1}d^{1,-}_{k,(l,m)} - (i\gamma^+_{l,m})^{n-k}(i\alpha_r)d^{3,+}_{k,(l,m)} + (-i\gamma^-_{l,m})^{n-k}(i\alpha_r)d^{3,-}_{k,(l,m)}\Big)$$
$$+\Big((i\gamma^+_{l,m})^{n-k-1}(i\alpha_r)d^{2,+}_{k,(l,m)} - (-i\gamma^-_{l,m})^{n-k-1}(i\alpha_r)d^{2,-}_{k,(l,m)} - (i\gamma^+_{l,m})^{n-k-1}(i\beta_s)d^{1,+}_{k,(l,m)}$$
$$+\,(-i\gamma^-_{l,m})^{n-k-1}(i\beta_s)d^{1,-}_{k,(l,m)}\Big)\,(iK_2(s-m))\Big]\,C_{n-k,(r-l,s-m)}e^{i(\alpha_r x+\beta_s y)}\,.$$

Finally, we exchange the sums in l,m and r,s to obtain the Fourier series for the right hand sides of (21) and (22). It is easily checked that

$$d^{i,\pm}_{k,(l,m)} = 0 \quad \text{if } |l|>kF \text{ or } |m|>kF.$$

Thus, the sums over (l,m) can be restricted to $-kF\leq l,m\leq kF$ and therefore the sums in (r,s) reduce to sums for $-nF\leq r,s\leq nF$. Then, equating Fourier coefficients yields the recursive formulae

$$d^{2,+}_{n,(r,s)} - d^{2,-}_{n,(r,s)} = -\left(A^2(-i\gamma)^n + A^3(-i\gamma)^{n-1}(iK_2 s)\right) C_{n,(r,s)} \tag{25}$$
$$- \sum_{k=0}^{n-1} \sum_{l=\max(-kF,r-(n-k)F)}^{\min(kF,r+(n-k)F)} \sum_{m=\max(-kF,s-(n-k)F)}^{\min(kF,s+(n-k)F)} \Big[(i\gamma^+_{l,m})^{n-k} d^{2,+}_{k,(l,m)} - (-i\gamma^-_{l,m})^{n-k} d^{2,-}_{k,(l,m)}$$
$$+ \left((i\gamma^+_{l,m})^{n-1-k} d^{3,+}_{k,(l,m)} - (-i\gamma^-_{l,m})^{n-1-k} d^{3,-}_{k,(l,m)}\right)(iK_2(s-m))\Big] C_{n-k,(r-l,s-m)}$$

and

$$\begin{aligned}
&\gamma^+_{r,s} d^{1,+}_{n,(r,s)} + \gamma^-_{r,s} d^{1,-}_{n,(r,s)} - \alpha_r d^{3,+}_{n,(r,s)} + \alpha_r d^{3,-}_{n,(r,s)} \\
&= -\left[-(\gamma A^1 + \alpha A^3)(-i\gamma)^n + (\alpha A^2 - \beta A^1)(-i\gamma)^{n-1}(iK_2 s)\right] C_{n,(r,s)} \\
&- \sum_{k=0}^{n-1} \sum_{l=\max(-kF,r-(n-k)F)}^{\min(kF,r+(n-k)F)} \sum_{m=\max(-kF,s-(n-k)F)}^{\min(kF,s+(n-k)F)} \Big[\gamma^+_{l,m}(i\gamma^+_{l,m})^{n-k} d^{1,+}_{k,(l,m)} \\
&+\gamma^-_{l,m}(-i\gamma^-_{l,m})^{n-k} d^{1,-}_{k,(l,m)} - (i\gamma^+_{l,m})^{n-k}\alpha_r d^{3,+}_{k,(l,m)} + (-i\gamma^-_{l,m})^{n-k}\alpha_r d^{3,-}_{k,(l,m)} \\
&+ \Big((i\gamma^+_{l,m})^{n-k-1}\alpha_r d^{2,+}_{k,(l,m)} - (-i\gamma^-_{l,m})^{n-k-1}\alpha_r d^{2,-}_{k,(l,m)} - (i\gamma^+_{l,m})^{n-k-1}\beta_s d^{1,+}_{k,(l,m)} \\
&+ (-i\gamma^-_{l,m})^{n-k-1}\beta_s d^{1,-}_{k,(l,m)}\Big)(iK_2(s-m))\Big] C_{n-k,(r-l,s-m)}\,.
\end{aligned} \tag{26}$$

A similar calculation for the second and fourth equations in (17) gives

$$d^{1,+}_{n,(r,s)} - d^{1,-}_{n,(r,s)} = -\left(A^1(-i\gamma)^n + A^3(-i\gamma)^{n-1}(iK_1 r)\right) C_{n,(r,s)} \tag{27}$$
$$- \sum_{k=0}^{n-1} \sum_{l=\max(-kF,r-(n-k)F)}^{\min(kF,r+(n-k)F)} \sum_{m=\max(-kF,s-(n-k)F)}^{\min(kF,s+(n-k)F)} \Big[(i\gamma^+_{l,m})^{n-k} d^{1,+}_{k,(l,m)} - (-i\gamma^-_{l,m})^{n-k} d^{1,-}_{k,(l,m)}$$
$$+ \left((i\gamma^+_{l,m})^{n-1-k} d^{3,+}_{k,(l,m)} - (-i\gamma^-_{l,m})^{n-1-k} d^{3,-}_{k,(l,m)}\right)(iK_1(r-l))\Big] C_{n-k,(r-l,s-m)}$$

and

$$\begin{aligned}
&\beta_r d^{3,+}_{n,(r,s)} - \beta_r d^{3,-}_{n,(r,s)} - \gamma^+_{r,s} d^{2,+}_{n,(r,s)} - \gamma^-_{r,s} d^{2,-}_{n,(r,s)} \\
&= -\left[(\gamma A^2 + \beta A^3)(-i\gamma)^n + (\alpha A^2 - \beta A^1)(-i\gamma)^{n-1}(iK_1 r)\right] C_{n,(r,s)} \\
&- \sum_{k=0}^{n-1} \sum_{l=\max(-kF,r-(n-k)F)}^{\min(kF,r+(n-k)F)} \sum_{m=\max(-kF,s-(n-k)F)}^{\min(kF,s+(n-k)F)} \Big[(i\gamma^+_{l,m})^{n-k}\beta_s d^{3,+}_{k,(l,m)} \\
&-(-i\gamma^-_{l,m})^{n-k}\beta_s d^{3,-}_{k,(l,m)} - \gamma^+_{l,m}(i\gamma^+_{l,m})^{n-k} d^{2,+}_{k,(l,m)} - \gamma^-_{l,m}(-i\gamma^-_{l,m})^{n-k} d^{2,-}_{k,(l,m)} \\
&+ \Big((i\gamma^+_{l,m})^{n-k-1}\alpha_r d^{2,+}_{k,(l,m)} - (-i\gamma^-_{l,m})^{n-k-1}\alpha_r d^{2,-}_{k,(l,m)} - (i\gamma^+_{l,m})^{n-k-1}\beta_s d^{1,+}_{k,(l,m)} \\
&+ (-i\gamma^-_{l,m})^{n-k-1}\beta_s d^{1,-}_{k,(l,m)}\Big)(iK_1(r-l))\Big] C_{n-k,(r-l,s-m)}\,.
\end{aligned} \tag{28}$$

On the other hand, the equations (18) are equivalent to

$$\alpha_r d^{1,+}_{n,(r,s)} + \beta_s d^{2,+}_{n,(r,s)} + \gamma^+_{r,s} d^{3,+}_{n,(r,s)} = 0 \tag{29}$$

and

$$\alpha_r d^{1,-}_{n,(r,s)} + \beta_s d^{2,-}_{n,(r,s)} + \gamma^-_{r,s} d^{3,-}_{n,(r,s)} = 0\,. \tag{30}$$

Thus, the six equations (25) to (30) allow us to compute the coefficients $\vec{d}^{\pm}_{n,(r,s)}$ in terms of $\vec{d}^{\pm}_{k,(l,m)}$, $k < n$, and $C_{j,(p,q)}$, and therefore give us the desired recursive formulae. Recursive formulae for a perfect conductor can be obtained from (25)-(30) simply by setting

$$d^{i,-}_{k,(l,m)} = 0 \quad \text{for } i = 1,2,3 \text{ and all } k,\, l \text{ and } m.$$

4 Numerical Results

In this section we present the results produced by our algorithm in some numerical experiments. The algorithm is fairly simple: it relies on the formulae (25)-(30) for the computation of the Taylor coefficients of the Rayleigh amplitudes and on *Padé approximation* (i.e. approximation by rational functions —see e.g. [1, 2, 3, 7, 13]) for the summation of the Taylor series, perhaps beyond their radii of convergence. This procedure is entirely analogous to that of the singly periodic case; we refer to [6] for details.

One point of interest in connection with our algorithm is that it produces the diffraction efficiencies *as functions of the height h/d*. In other words, once the Taylor coefficients and the Padé approximants for a particular wavelength and period have been found, calculation of efficiencies for any particular height reduces to evaluation of simple rational functions. This feature, of which we have taken advantage in the examples that follow, is significant in design applications, in which many numerical experiments must be performed in the search for a particular behavior of the device under consideration.

As we have said, our algorithm can yield good performance with limited requirements in terms of computing power. For a surface which can be represented accurately by a double Fourier series of order $m \times m$ and if approximations of order n are sought, the storage requirement is of the order of m^2n^3 locations. The corresponding computing time is of the order of n^6. While the computing time could seem quite elevated, it is not so in practice, as very good convergence can be obtained for rather small values of n, see Tables 4 and 5. For example, a calculation with $n = 13$ for a bi-sinusoidal grating can be performed in about 20 to 30 seconds in a Sparc station IPX. Corresponding times for $n = 17$, 21, 25, 29 and 33 in the problem of Table 4 are 1.5 min, 5 min, 14.5 min, 34.5 min, and 75 min respectively.

For simplicity, we shall restrict ourselves to sinusoidal bigratings of the form

$$f(x,y) = \frac{h}{4}\left[\cos\left(\frac{2\pi x}{d}\right) + \cos\left(\frac{2\pi y}{d}\right)\right], \tag{31}$$

i.e. $F = 1$ in (20). In our first example, Table 1, we present the computed values of the reflected efficiencies (cf. (7)), as a function of the height-to-period ratio, for a *perfectly conducting* grating illuminated under normal incidence with light of wavelength-to-period ratio $\lambda/d = 0.83$. The number ϵ denotes the defect in the energy relation (8)

$$\epsilon = 1 - \left[\sum_{(r,s)\in U^+} e^+_{r,s} + \sum_{(r,s)\in U^-} e^-_{r,s}\right].$$

(In the case of a perfectly conducting grating we have, of course, $e^-_{r,s} = 0$.)

h/d	$e_{(-1,0)}$	$e_{(0,-1)}$	$e_{(0,0)}$	ϵ
0.1	0.018810	0.059691	0.842996	-6.6E-16
0.2	0.063551	0.192968	0.486961	-2.5E-15
0.3	0.110711	0.308565	0.161448	-6.0E-13
0.4	0.139786	0.342547	0.035335	-9.2E-10
0.5	0.134627	0.283651	0.163443	-1.6E-07
0.6	0.089612	0.168376	0.484016	-7.1E-06
0.7	0.036325	0.068458	0.790359	-7.1E-05
0.8	0.035293	0.033719	0.862052	7.8E-05
0.9	0.097266	0.040570	0.727476	3.1E-03
1.0	0.180165	0.048574	0.557739	1.5E-02

Table 1: Efficiencies for the perfectly conducting sinusoidal grating (31) under normal incidence with a wavelength-to-period ratio $\lambda/d = 0.83$: [14/14] Padé approximants.

In the problem considered in Table 1 there are five propagating modes with $e_{(1,0)} = e_{(-1,0)}$ and $e_{(0,1)} = e_{(0,-1)}$. We observe an excellent performance of the method, with meaningful results for height-to-period ratios of up to $h/d = 1$.

Applications of other numerical methods for crossed gratings have been restricted, due to constraints in computing time and storage, to cases in which only a few non-evanescent modes occur. Our method does not seem to be affected by such problems, and it remains accurate even in the presence of a large number of diffracted modes. To illustrate this point, we present in Table 2 results corresponding to normal incidence of light with $\lambda/d = 0.4368$ (a case which has been used repeatedly in the literature in tests of numerical methods for singly periodic gratings). In this case there are 21 diffracted modes, and we have chosen to display the efficiency in the $(0,0)$ order only. A very good performance is still observed.

h/d	$e_{0,0}$	ϵ
0.1	0.583991	5.9E-15
0.2	0.086946	2.1E-14
0.3	0.000351	5.5E-13
0.4	0.006391	1.4E-08
0.5	0.065342	2.9E-06
0.6	0.087383	-2.8E-04
0.7	0.164344	-6.0E-03
0.8	0.150834	2.6E-02

Table 2: Efficiency of order $(0,0)$ for the perfectly conducting grating (31) under normal incidence with a wavelength-to-period ratio $\lambda/d = 0.4368$: [14/14] Padé approximants.

In order to gain an insight on the performance of the method in transmission problems, we present, in Table 3, data corresponding to the same case as in Table 1 except that now the grating is made from a material with a real refractive index $\nu_0 = 2$. Only the values of the efficiencies corresponding to reflected orders are shown. We see that the accuracy in this loseless transmission problem is at most one order of magnitude worse than in the perfect conductor case.

h/d	$e_{(-1,0)}$	$e_{(0,-1)}$	$e_{(0,0)}$	ϵ
0.1	3.27740E-03	3.72963E-03	9.62746E-02	1.8E-14
0.2	1.04422E-02	1.18396E-02	6.17586E-02	1.5E-14
0.3	1.59870E-02	1.82072E-02	2.77715E-02	-1.0E-11
0.4	1.62416E-02	1.90710E-02	7.76777E-03	-7.1E-09
0.5	1.17477E-02	1.50841E-02	1.97567E-03	1.7E-07
0.6	5.95943E-03	9.39648E-03	2.96947E-03	6.4E-05
0.7	1.99679E-03	4.60557E-03	4.12865E-03	1.0E-03
0.8	6.48092E-04	1.78457E-03	3.45135E-03	8.8E-03
0.9	1.02779E-03	3.79257E-04	2.02366E-03	3.8E-02
1.0	2.17608E-03	5.75382E-05	1.05870E-03	1.1E-01

Table 3: Efficiencies for the sinusoidal grating (31) with index of refraction $\nu_0 = 2$, under normal incidence with a wavelength-to-period ratio $\lambda/d = 0.83$: [14/14] Padé approximants.

For comparison purposes, we now give three examples that correspond to the lossy gratings treated in [18]. The values for the refractive indices of metals we used were taken from [21]. The first two cases below (Figures 1 and 2) were obtained in [18] as a result of a search for totally absorbing gratings. For this, the authors considered first a bi-sinusoidal grating in gold and studied the zeroth-order reflectance as a function of the period d (see [18, Fig. 7.17]). Only the zero order efficiency is non-evanescent in this case.

In Figure 1 we show the results given in this case by our algorithm. Qualitative agreement with the results in [8, 18] is observed. However, some discrepancies do occur. For example, in contrast with Figure 7.17 of [18], our curves 2 and 3 coincide at $d = 0.62\mu$m. This prompted us to analyze the accuracy of our results. We found that, for this range of parameters, our method yields extremely accurate results, with errors in the reflected energy ("E. R.") which are better than 10^{-14}. This can be seen in Table 4, which contains a convergence study for the values of the reflected energy at $d = 0.62\mu m$ for the curves labeled 2 and 3 in Figure 1. We see that, as claimed, an accuracy better than 8 digits is obtained by an approximation of order 13. To demonstrate the range of parameters in which our method can be applied, we include a third column in Table 4 showing the values of E. R. for a much deeper grating profile of height $h = 0.500\mu$m, for which $h/d = 0.806$. We see

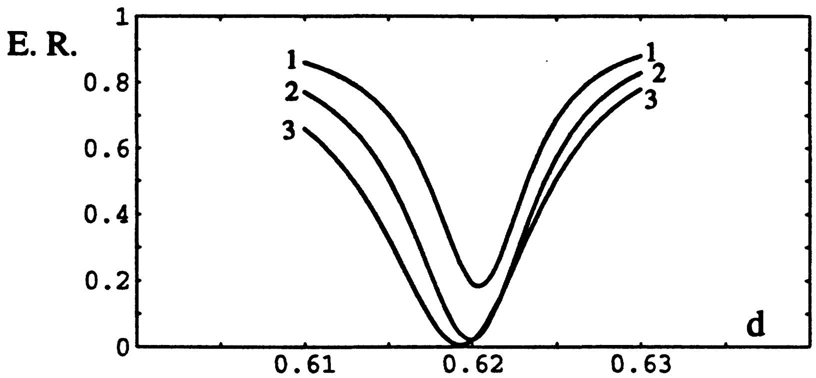

Figure 1: Energy reflected by a sinusoidal grating in gold used with normally incident light of wavelength $0.65\mu m$. 1. $h = 0.040\mu m$; 2. $h = 0.055\mu m$; 3. $h = 0.070\mu m$: [6/6] Padé approximants

that even in this case, the results are quite accurate: the errors are of the order of 10^{-4} for a [6/6] approximant ($n = 13$) and of 10^{-6} for a [14/14] approximant ($n = 29$) (Padé approximants with n=15, 19, 23, 27 and 31 are singular for this problem.) The computing time used for the calculation of the Taylor coefficients and the corresponding Padé approximants with $n = 13$ was of about twenty seconds in a Sparc station IPX. As pointed out above, particular calculations for several values of the height take virtually no computer time once the Padé approximants have been found. We find the results in the first row of Table 4 rather satisfactory, and even more so taking into account the limited computer power they required. The accuracy of the integral method in this problem ($h = 0.055$ and $h = 0.070$) has been estimated to be of the order of two digits [8].

n	$h = 0.055\mu m$	$h = 0.070\mu m$	$h = 0.500\mu m$
13	0.0227882361359963	0.0226057361431067	0.84146746
17	0.0227882361334883	0.0226057359874209	0.84202623
21	0.0227882361334891	0.0226057359874838	0.84219841
25	0.0227882361334900	0.0226057359874644	0.84260919
29	0.0227882361334896	0.0226057359874220	0.84197301
33	0.0227882361334896	0.0226057359874253	0.84197398

Table 4: Convergence study of the reflected energy for the example in Figure 1 (gold). The period is fixed at 0.62μm and the wavelength at 0.65μm. $[\frac{n-1}{2}/\frac{n-1}{2}]$ Padé approximants.

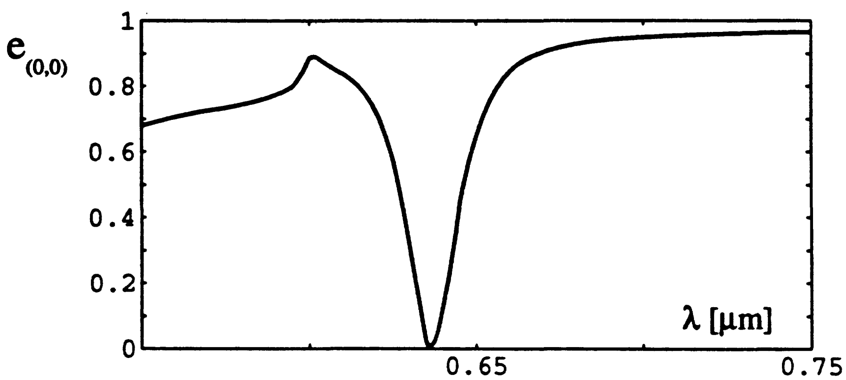

Figure 2: Zeroth-order efficiency for a sinusoidal grating in gold having a groove depth $h = 0.080\mu$m and a period of 0.60μm, used with normally incident light: [6/6] Padé approximants

From Figure 1 we see that, as established in [8, 18], the grating is highly absorbing when the period d is close to $d = 0.62\mu$m. Indeed, when the period is fixed to $d = 0.62\mu$m our code reveals that the reflected energy attains a minimum at $h = 0.0620 \pm 0.0001$, where E. R.= 0.007. As mentioned above this value can be computed with great accuracy. Such high accuracies are required in some applications [15, p. 46], [17, p. 218].

Similar values of the parameters were used to produce Figure 7.18 in [18]. The groove depth was fixed at $h = 0.080\mu$m and the period at $d = 0.60\mu$m, while the wavelength was varied between $0.55\mu m$ and $0.75\mu m$. In Figure 2 we display the results given by our algorithm; our graph appears to coincide with [18, Fig. 7.18].

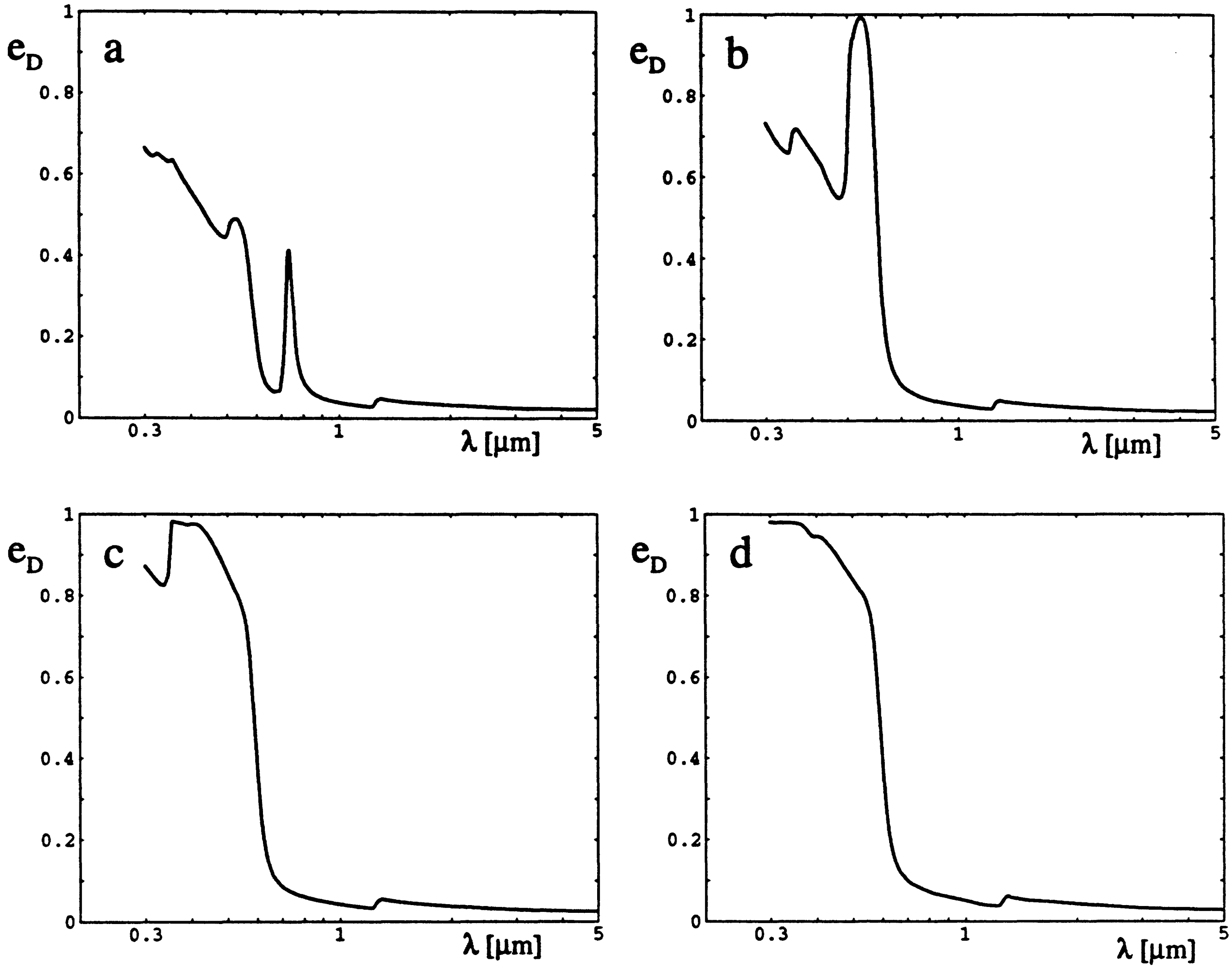

Figure 3: The energy absorbed by a sinusoidal grating in copper having a groove depth $h = 0.20\mu$m as a function of the wavelength for normally incident light. (a) $d = 0.7071\mu$m; (b) $d = 0.50\mu$m; (c) $d = 0.35\mu$m; (d) $d = 0.20\mu$m: [6/6] Padé approximants

Finally, Figure 3 is related to the study of the reduction of metallic reflectivity given in [18]. The objective is to construct a solar selective grating which is highly absorbing throughout the visible region and highly reflecting in the near infrared. The results of our code for a sinusoidal grating in copper are plotted in Figure 3 (see [18, Fig. 7.19]). While the general features of these curves are similar to those in [18, Fig. 7.19], comparison shows that our graphs differ from those there in a number of important details. For example, in [18, Fig. 7.19] the absorbed energy in Figures 3a,b is below our predictions, for the shortest wavelengths, by as much as 20%. This is probably due either to low accuracies in the results given by the integral method, or to differences in the values used of the refractive index of copper. The accuracy of our predictions is shown by the convergence study of Table 5.

n	$d = 0.7071\mu m$	$d = 0.5000\mu m$
13	0.66407973570	0.73248902890
17	0.66442364189	0.72911437001
21	0.66442218058	0.72918754870
25	0.66442216062	0.72919146502
29	0.66442215270	0.72919155477
33	0.66442215271	0.72919154229

Table 5: Convergence study of the absorbed energy for the example in Figures 3(a) and 3(b) (copper). The wavelength is fixed at $\lambda = 0.3\mu$m and the period at $d = 0.7071\mu$m for Figure 3(a) and at $d = 0.5000\mu$m for Figure 3(b). $[\frac{n-1}{2}/\frac{n-1}{2}]$ Padé approximants.

Conclusions:

We have introduced a new numerical method for the solution of problems of diffraction in a doubly periodic, three dimensional structure. The method is based on a rigorous high order perturbative technique which had proven successful in the corresponding problems in the singly periodic case. If approximations of very high order are sought, our method may become prohibitively expensive in terms of computing time and storage. Fortunately, however, excellent convergence is observed for approximations of relatively low orders. Furthermore, once the Padé approximants have been calculated for a particular set of parameters, the efficiencies can be obtained for any number of different heights at virtually no cost. And, the performance does not seem to be substantially affected by the presence of a large number of non-evanescent modes.

We have shown through examples of varied nature that computation times of about twenty to thirty seconds on a desk top computer suffice to give very accurate results for bisinusoidal gratings. Generalization of our codes to surfaces other than bi-sinusoidal is in principle immediate, but the full domain of applicability of our algorithm is yet to be explored.

We have compared our results with other theoretical results available in the literature. The most important features of the efficiency curves given by other methods, such as total absorption, have been confirmed. Some rather marked differences have been observed, however, between previous curves and ours. Thus we have performed convergence studies which demonstrated the high accuracy of our results; graphical differences can therefore be attributed to low accuracies of other methods, or to use of different values for the refractive indices of the metals. In any case, the higher resolution of our method has been established. We believe that the improvement in the numerical resolution given by our algorithm, accompanied by its low computational cost, will prove significant in future design applications.

Acknowledgments. OB gratefully acknowledges support from NSF through grant No. DMS-9200002. This work was partially supported by the Army Research Office and the National Science Foundation through the Center for Nonlinear Analysis.

References

[1] Baker, G. A. and Graves–Morris, P., *Padé Approximants. Part I: Basic Theory,* Addison–Wesley, Massachusetts (1981).

[2] Baker, G. A. and Graves–Morris, P., *Padé Approximants. Part II: Extensions and Applications,* Addison–Wesley, Massachusetts (1981).

[3] Brezinski, C., *Procedures for estimating the error in Padé approximation,* Mathematics of Computation **53**, 639–648 (1965).

[4] Bruno, O. P. and Reitich, F., *Solution of a boundary value problem for Helmholtz equation via variation of the boundary into the complex domain,* Proc. Roy. Soc. Edinburgh **122A**, 317–340.

[5] Bruno, O. P. and Reitich, F., *Numerical solution of diffraction problems: a method of variation of boundaries,* to appear in J. Opt. Soc. Amer. A.

[6] Bruno, O. P. and Reitich, F., *Numerical solution of diffraction problems: a method of variation of boundaries II. Dielectric gratings, Padé approximants and singularities,* Preprint (1992).

[7] Cabay, S. and Choi, D., *Algebraic computations of scaled Padé fractions,* SIAM J. Comput. **15**, 243–270 (1986).

[8] Derrick, G. H., McPhedran, R. C., Maystre, D. and Neviére, M., *Crossed Gratings: a theory and its applications,* Appl. Phys. **18**, 39–52 (1979).

[9] Dobson, D. C. and Friedman, A., *The time-harmonic Maxwell equations in a doubly periodic structure,* J. Math. Anal. Appl. **166**, 507–528 (1992).

[10] D. C. Dobson, and J. A. Cox, *An integral equation method for biperiodic diffraction structures,* SPIE **1545**, 106–113 (1991).

[11] Fan, J. C. C., Bachner, F. J., and Murphy, R. A., *Thin-film conducting microgrids as transparent heat mirrors,* Appl. Phys. Let. **28**, 440–442 (1976).

[12] Glytsis, E. N. and Gaylord, T. K., *Three-dimensional (vector) rigorous coupled-wave analysis of anisotropic grating diffraction,* J. Opt. Soc. Amer. A **7**, 1399–1420 (1990).

[13] Graves–Morris, P., *The numerical calculation of Padé approximants,* Lecture Notes in Mathematics **765**, ed. L. Wuytack, 231–245 (1979).

[14] Horwitz, C. M., *A new solar selective surface,* Opt. Commun. **11**, 210–212 (1974).

[15] Maystre, D., *Rigorous vector theories of diffraction gratings,* in Progress in Optics, ed. E. Wolf, North Holland, Amsterdam (1984).

[16] Maystre, D. and Nevière, M., *Electromagnetic theory of crossed gratings,* J. Optics **9**, 301–306 (1978).

[17] Maystre, D., Nevière, M., and Petit, R. *Experimental verifications and applications of the theory,* in Electromagnetic Theory of Gratings, ed. R. Petit, Springer, Berlin (1980).

[18] McPhedran, R. C., Derrick, G. H and Botten, L. C., *Theory of Crossed Gratings,* in Electromagnetic Theory of Gratings, ed. R. Petit, Springer, Berlin (1980).

[19] Gaylord, T. K. and Moharam, M. G., *Analysis and applications of optical diffraction by gratings,* Proc. IEEE **73**, 894–937 (1985).

[20] Müller, C., *Foundations of the Mathematical Theory of Electromagnetic Waves,* Springer, Berlin (1969).

[21] Palik, E. D., Ed., *Handbook of optical constants of solids,* Academic Press, Orlando, (1985).

[22] Petit, R., *A tutorial introduction,* in Electromagnetic Theory of Gratings, ed. R. Petit, Springer, Berlin (1980).

[23] Uretsky, J. L., *The scattering of plane waves from periodic surfaces,* Ann. Phys. **33**, 400–427 (1965).

[24] Vincent, P., *A finite difference method for dielectric and conducting crossed gratings,* Opt. Commun. **26**, 293–296 (1978).